Articles

N-Methylated Cyclic RGD Peptides as Highly Active and Selective $\alpha_V\beta_3$ Integrin Antagonists

Michael A. Dechantsreiter,† Eckart Planker,† Barbara Mathä,† Elisabeth Lohof,† Günter Hölzemann,‡ Alfred Jonczyk,‡ Simon L. Goodman,‡ and Horst Kessler*,†

Institut für Organische Chemie und Biochemie, Technische Universität München, Lichtenbergstrasse 4, D-85747 Garching, Germany, and Merck KGaA Preclinical Research, Frankfurter Strasse 250, D-64271 Darmstadt, Germany

Received March 11, 1999

The $\alpha_V\beta_3$ integrin receptor plays an important role in human tumor metastasis and tumor-induced angiogenesis. The in vivo inhibition of this receptor by antibodies or by cyclic peptides containing the RGD sequence may in the future be used to selectively suppress these diseases. Here we investigate the influence of *N*-methylation of the active and selective $\alpha_V\beta_3$ antagonist cyclo(RGDfV) (**L1**) on biological activity. Cyclo(RGDf-N(Me)V-) (**P5**) was found to be even more active than **L1** and is one of the most active and selective compounds in inhibiting vitronectin binding to the $\alpha_V\beta_3$ integrin. Its high-resolution, three-dimensional structure in water was determined by NMR techniques, distance geometry calculations, and molecular dynamics calculations, providing more insight into the structure−activity relationship.

Introduction

Cyclic RGD pentapeptides have been developed in our group as highly active and selective ligands for the $\alpha_V\beta_3$ integrin receptor.[1−3] A "spatial screening" procedure[4,5] led to cyclo(RGDfV) (**L1**), the first highly active and selective $\alpha_V\beta_3$ antagonist, which now serves as a lead structure for the development of stereoisomeric libraries[6,7] and peptidomimetics.[8,9] Selective inhibition of the $\alpha_V\beta_3$ receptor is also achieved with the monoclonal antibody LM609 as well as with nonpeptidic antagonists of the 1,4-benzodiazepine type.[10]

The $\alpha_V\beta_3$ receptor, a member of the integrin family, is involved in many cell-matrix recognition and cell-adhesion phenomena. It plays an important role in angiogenesis[11] (the outgrowth of new blood vessels). The $\alpha_V\beta_3$ integrin is expressed on the surface of a variety of cell types, including osteoclasts, vascular smooth muscle cells, endothelial cells, and certain tumor cells. In tumor-induced angiogenesis, invasive endothelial cells bind via this integrin to extracellular matrix components. The inhibition of this interaction induces apoptosis[12,13] of the proliferative angiogenic vascular cells. The $\alpha_V\beta_3$ integrin receptor is also involved in cell migration and is upregulated during the vertical growth phase and metastasis of malignant melanoma cells, whereas integrins which establish tight contacts during tissue organization may be downregulated in tumor cells.[14,15]

N-Methylation of the peptide backbone has been shown to be a valuable tool in structure−activity relationship studies.[16−18] It is known from $\alpha_{IIb}\beta_3$ antagonistic cyclic RGD peptides that N^{α}-methylation of the arginine residue leads to conformationally more constrained analogues and is particulary important for obtaining high binding affinity.[19,20] In addition, incorporation of N^{α}-methylated amino acids into different biologically important peptides has led to analogues with improved pharmacological properties, such as enhanced potency and duration of action, attributed to their increased stability or has led to conversion of an agonist into an antagonist.[21,22] The exchange of a *N*-methylated, D,L-configurated dipeptide unit in a cyclic peptide for a L,L-dipeptide unit has resulted in a change of selectivity from an $\alpha_{IIb}\beta_3$-selective substance to an $\alpha_V\beta_3$-selective peptide.[23] With the synthesis of a series of five *N*-methylated cyclic peptides (Figure 1) we investigated if *N*-methylation of a single peptide bond in the lead structure **L1** has similar positive effects on activity and selectivity. Every amide bond was replaced sequentially by the corresponding *N*-methylated unit. This methylation scan has provided the new lead compound cyclo(RGDf-N(Me)V-) (**P5**) with enhanced biological activity in the subnanomolar range. This compound (code EMD121974, Merck KGaA, Darmstadt, Germany) is currently in clinical studies against Kaposi's sarcoma, brain tumors, and solid tumors.

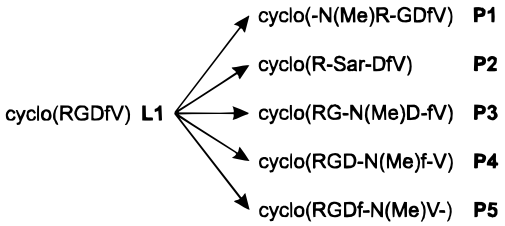

Figure 1. Series of *N*-methylated cyclic peptides derived from cyclo(RGDfV).

* Author for correspondence: Prof. Dr. H. Kessler. Tel: ++49-89-289 13301. Fax: ++49-89-289 13210. E-mail: Kessler@ch.tum.de.
† Technische Universität München.
‡ Merck KGaA Preclinical Research.

10.1021/jm970832g CCC: $18.00
Published on Web 07/24/1999

Results

Chemistry. Several methods for *N*-methylation of amino acids are known in the literature.[24−26] Following the Fmoc strategy in peptide synthesis, the method of *Freidinger et al.* is most favorable as it results in *N*-methylated Fmoc-protected amino acids in good overall yields without racemization. *N*-Methylation is achieved by condensation of the Fmoc-protected amino acid with paraformaldehyde, resulting in an oxazolidinone which can be opened under acidic, reductive conditions to give the desired *N*-methyl amino acid. The derivatives of valine and D-phenylalanine were synthesized according to this procedure. Fmoc-N(Me)Arg(Mtr)-OH was prepared by *N*-Boc deprotection of commercially available Boc-N(Me)Arg(Mtr)-OH and subsequent Fmoc protection using standard conditions. Fmoc-N(Me)Asp-(OtBu)-OH and Fmoc-Sar-OH are commercially available.

The linear, side-chain-protected peptides were assembled with the glycine residue at the C-terminus (peptides **P1**, **P2**, **P4**, and **P5**) to prevent racemization and steric hindrance during the cyclization step. Only in the case of **P3** the sequence of the linear peptide was varied to H-Gly-N(Me)Asp(OtBu)-D-Phe-Val-Arg(Pbf)-OH to avoid cyclization between the N-terminal *N*-methylated aspartic acid residue and the C-terminal glycine residue. The synthesis was performed using Merrifield solid-phase peptide techniques[27,28] with *o*-chlorotrityl chloride (cTrt) resin applying Fmoc strategy.[29] The Fmoc-protected amino acids were coupled with *O*-(1*H*-benzotriazol-1-yl)-*N*,*N*,*N*′,*N*′-tetramethyluronium tetrafluoroborate (TBTU), 1-hydroxybenzotriazole (HOBt), and diisopropylethylamine (DIEA) as base. In the case of **P1** and **P3**, the coupling of glycine and valine to the corresponding *N*-methylated amino acids was achieved with HOAt and HATU. Especially in the case of peptide **P1**, no other coupling reagent, either in solution or using SPPS, was successful. The linear peptides were obtained with over 90% yield. Cyclization was carried out at high dilution (1.25×10^{-3} M) in DMF via in situ activation using diphenyl phosphorazidate (DPPA) with sodium bicarbonate as solid base[30] (**P2** and **P3**) or TBTU, HOBt, and DIEA as cyclization reagents (**P1**, **P4**, and **P5**). Final deprotection was achieved with trifluoracetic acid (TFA) and scavengers (ethanedithiol). Purification by reversed-phase high-performance liquid chromatography (RP-HPLC) yielded peptides which were >98% pure. All peptides were characterized by ESI and high-resolution mass spectroscopy as well as various NMR techniques.

Biological Data. The ability of RGD peptides to inhibit the binding of vitronectin and fibrinogen to the isolated, immobilized $\alpha_{IIb}\beta_3$ and $\alpha_V\beta_3$ receptors was compared with that of the linear standard peptide GRGDSPK and with that of **L1**. To obtain intra-assay comparable results, normalized activities given as the ratio $Q = IC_{50}$[peptide]/IC_{50}[GRGDSPK] were used. In case of the $\alpha_V\beta_3$ receptor the peptides **P3** and **P4** show a lower activity than the linear standard and **P1**. Peptides **P1**, **P2**, and **P5** show an increased activity compared to the linear standard peptide. **P1** is about as active as **L1**. Interestingly, cyclo(R-Sar-DfV) (**P2**) shows only an 18-fold lower activity than the lead structure **L1**. Sarcosine with its *N*-methyl group can be considered as the peptoid analogue monomer of alanine with the shifted side chain from the C_α to the nitrogen atom.[31] This biological activity for **P2** is unexpected, because incorporation of alanine or β-alanine instead of glycine in the RGD sequence leads to a complete loss of activity.[32] Only **P5** (IC_{50} of 0.58 nM) reveals a higher activity than **L1** (4-fold) and is about 2400-fold more active than **P4**. On the other hand, all cyclic RGD peptides show only low activities in inhibiting fibrinogen binding to the $\alpha_{IIb}\beta_3$ receptor. The most active peptide is **P5**, which is about 2-fold more active to $\alpha_V\beta_3$ than the linear standard peptide. Considering the selectivity between the $\alpha_{IIb}\beta_3$ and $\alpha_V\beta_3$ receptors, peptide **P5** shows a 1500-fold higher activity for vitronectin binding to $\alpha_V\beta_3$ than fibrinogen binding to $\alpha_{IIb}\beta_3$. It is the most selective antagonist of this series, even compared to **L1**. The IC_{50} and *Q* values of the cyclic peptides and the standard peptides toward the $\alpha_{IIb}\beta_3$ and $\alpha_V\beta_3$ receptor are given in Table 1.

Table 1. IC_{50} and *Q* Values of *N*-Methylated Cyclic Peptides and Standard Peptides

peptide	$\alpha_V\beta_3$		$\alpha_{IIb}\beta_3$	
	IC_{50} (μM)	*Q*	IC_{50} (μM)	*Q*
GRGDSPK	0.21	1.0	1.7	1.0
L1, cyclo(RGDfV), TFA	0.0025	0.012	1.7	1.0
P1, cyclo(-N(Me)R-GDfV)	0.0055	0.026	5.2	3.1
P2, cyclo(R-Sar-DfV)	0.045	0.21	>10	>5.9
P3, cyclo(RG-N(Me)D-fV)	0.56	2.7	>10	>5.9
P4, cyclo(RGD-N(Me)f-V)	1.4	6.7	>10	>5.9
P5, cyclo(RGDf-N(Me)V-)	0.00058	0.0028	0.86	0.51

Table 2. Proton and Carbon Chemical Shifts of **P5** in H_2O at 301 K

residue	chemical shifts (ppm)					
	H^N	H^α	H^β	H^γ	H^δ	H^ϵ
Arg[1]	8.28	4.08	1.95	1.61	3.22/3.26	7.27
Gly[2]	8.01	3.59^{proR} 4.14^{proS}				
Asp[3]	8.47	4.61	2.58^{proS} 2.75^{proR}			
D-Phe[4]	8.12	5.26	3.08		7.34	
Val[5]	$2.90^{N(CH_3)}$	4.35	2.08	0.56^{proS} 0.90^{proR}		
			C^α	C^β	C^γ	C^δ
Arg[1]			57.4	28.3	28.0	43.4
Gly[2]			46.3			
Asp[3]			54.0	39.8		
D-Phe[4]			53.8	40.1		43.4
Val[5]	33.7^{NC}		67.3	28.7	21.3	

Structure Determination. Due to the pharmacological potential of **P5,** its three-dimensional structure in water was determined by NMR spectroscopy, metric matrix distance geometry (DG) calculations, and molecular dynamics (MD) simulations. A complete assignment of the proton and carbon resonances could be obtained (Table 2). The prochiral methylene protons of glycine and aspartate as well as the valine methyl protons were assigned by the corresponding $^3J(H^N,H^\alpha)$ and $^3J(H^\alpha,H^\beta)$ coupling constants and by testing both prochiral assignments for NOE restraint violations during MD simulations.

The proton−proton distances were calculated from both the NOESY and ROESY spectra measured with a mixing time of 100 ms. The isolated spin pair approximation was used, setting the integrated intensity

of the glycine geminal pair of protons to a distance of 1.78 Å. The regions above and below the diagonal of the NOESY and ROESY were analyzed separately, yielding a set of four distances for each pair of protons. The standard lower and upper bounds of the distance restraints were then set to $L = \langle D \rangle - 0.1\langle D \rangle$, $U = \langle D \rangle + 0.1\langle D \rangle$ ($\langle D \rangle$ = average of the distance set). However, if an experimental value (out of the set of four) was outside these assumed minimal error margins, it was taken to substitute the error margin to account for the experimental uncertainties. During the MD calculations distances to equivalent and degenerated protons were calculated as the r^{-6} sum.[33]

The $^3J(H^N,H^\alpha)$ coupling constants of Gly^2 and Asp^3 were not used as dihedral angle restraints because cyclic pentapeptides usually show flexibility at this position. The results of this work confirmed this to be the case for **P5** as well, although to a smaller extent. Additionally, distance restraints that would apparently lead to distorted conformations due to multirotamers of the side chains were excluded from the set of restraints used in the structure calculations. In the final analysis of the structure they were included again assuming the adopted side-chain rotmers of Arg^1, Asp^3, and Phe^4 to be equally populated (see below and footnote b of Table 3). Two $^3J(H^N,H^\alpha)$ coupling constants and 39 proton−proton distances were applied in the DG and restrained MD calculations (Tables 3 and 4).

First, DG calculations[34] were carried out providing the most complete and the least biased search of conformational space. More than 70 of the 100 DG structures did not show any significant violation of the applied NMR-derived restraints and were highly ordered. Only the orientation of the amide groups connected to glycine varied about 90°. Since DG structures are based only on molecular connectivities and experimental constraints, and hence often show slight distortions, the average structure of the 20 best was chosen as representative and subjected to further refinement. Additional empirical constraints of a force field are applied in MD simulations which we carried out in explicit solvent H_2O. The averaged and energy-minimized structure from the restrained MD trajectory, recorded for 100 ps at 300 K, is displayed in Figure 2. Additionally, to obtain more insight in the conformational flexibility of the cyclic peptide **P5**, a 400-ps MD simulation at 300 K was carried out in explicit H_2O without applying any experimental restraints (free MD). During the free MD calculation the structure remained stable and very similar to the structure from the restrained simulation. The distance RMSD between the average structures from both the free and restrained simulations is 0.25 Å for the backbone atoms. This excellent agreement proves that the solution structure calculated from NMR data represents a stable low-energy conformer.

Cyclic pentapeptides of the LDLDL-series usually exhibit a βII'/γ conformation with the D-amino acid residues preferably at the $i+1$ positions of the turns.[2,35] Since glycine can act as a D-amino acid, cyclo(RGDfV) (**L1**) also adopts this typical conformation.[5] Moreover, it is more or less common for cyclic pentapeptides to show considerable flexibility in the γ turn, leading to strong violations of NMR-derived restraints.[35,36] The dynamics of cyclic pentapeptides can be compared with the rapid pseudorotation of cyclopentane.[4]

Table 3. Distance Restraints and Their Violations from the Restrained MD Simulation of **P5** in H_2O

proton 1	proton 2	lower bound (Å)	upper bound (Å)	calcd distance (Å)	violation (Å)
Arg^1 H^N	Arg^1 H^α	2.17	3.00	2.99	0.00
Arg^1 H^N	Arg^1 H^β	2.63	3.22	2.74[a,b]	0.00
Arg^1 H^N	Arg^1 H^γ	2.71	3.46	3.17[a,b]	0.00
Arg^1 H^α	Arg^1 H^β	2.17	2.65	2.39[a,b]	0.00
Arg^1 H^α	Arg^1 H^γ	2.24	2.82	2.65[a,b]	0.00
Arg^1 H^β	Arg^1 H^δ	1.99	2.43	2.15[a]	0.00
Arg^1 H^N	Gly^2 H^N	3.13	3.83	3.55	0.00
Arg^1 H^N	Val^5 H^α	2.46	3.42	3.46	0.04
Arg^1 H^N	Val^5 H^β	2.66	3.49	2.66	0.00
Arg^1 H^N	Val^5 $C^{proR}H^\gamma$	2.86	3.70	3.64[a]	0.00
Arg^1 H^N	Val^5 N(CH_3)	2.62	3.20	2.73[a]	0.00
Arg^1 H^γ	Val^5 $C^{proR}H^\gamma$	2.22	3.06	3.24[a,b]	0.18
Gly^2 H^N	Arg^1 H^α	2.43	3.23	2.42	−0.02
Gly^2 H^N	Arg^1 H^β	2.99	4.10	4.42[a,b]	0.32
Gly^2 H^N	Arg^1 H^γ	4.09	5.00	4.59[a,b]	0.00
Gly^2 H^N	Gly^2 $H^{\alpha proR}$	2.42	3.29	2.60	0.00
Gly^2 H^N	Gly^2 $H^{\alpha proS}$	2.75	3.61	3.10	0.00
Gly^2 H^N	Val^5 N(CH_3)	3.85	5.03	5.32[a]	0.29
Asp^3 H^N	Gly^2 $H^{\alpha proR}$	2.60	3.73	3.50	0.00
Asp^3 H^N	Gly^2 $H^{\alpha proS}$	2.41	3.28	2.40	−0.01
Asp^3 H^N	Asp^3 H^α	2.56	3.13	3.02	0.00
Asp^3 H^N	Asp^3 $H^{\beta proS}$	2.77	3.76	2.73[b]	−0.04
Asp^3 H^N	Asp^3 $H^{\beta proR}$	2.97	4.01	2.84[b]	−0.13
Asp^3 H^N	Phe^4 H^N	3.55	4.60	3.79	0.00
Asp^3 H^N	Val^5 N(CH_3)	3.84	4.80	4.93[a]	0.12
Phe^4 H^N	Gly^2 $H^{\alpha proR}$	3.92	4.79	4.77	0.00
Phe^4 H^N	Asp^3 H^α	2.15	2.63	2.38	0.00
Phe^4 H^N	Asp^3 $H^{\beta proS}$	3.81	4.65	4.62[b]	0.00
Phe^4 H^N	Asp^3 $H^{\beta proR}$	3.71	4.53	4.39[b]	0.00
Phe^4 H^N	Phe^4 H^α	2.75	3.49	3.05	0.00
Phe^4 H^N	Phe^4 H^β	2.27	2.95	2.93[a,b]	0.00
Phe^4 H^N	Phe^4 H^δ	3.34	4.26	3.60[a,b]	0.00
Phe^4 H^α	Phe^4 H^β	2.15	3.01	2.38[a,b]	0.00
Phe^4 H^N	Val^5 H^α	4.20	5.13	4.77	0.00
Phe^4 H^N	Val^5 N(CH_3)	3.27	4.35	4.42[a]	0.08
Phe^4 H^α	Val^5 N(CH_3)	2.10	2.76	2.50[a]	0.00
Phe^4 H^β	Phe^4 H^δ	2.11	2.57	2.19[a]	0.00
Val^5 H^α	Val^5 H^β	2.63	3.36	3.02	0.00
Val^5 H^α	Val^5 $C^{proR}H^\gamma$	2.20	3.02	3.04[a]	0.02
Val^5 H^α	Val^5 $C^{proS}H^\gamma$	2.21	2.86	2.85[a]	0.00
Val^5 H^β	Val^5 N(CH_3)	1.92	2.45	2.51[a]	0.06

[a] Distance calculated as r^{-6} sum. [b] r^{-6} average over two side-chain conformations assumed to be equally populated (as indicated by the coupling constants). The side-chain rotamers are χ_1 = 180°/−60° for Arg and Asp and χ_1 = 180°/+60° for D-Phe, respectively.

P5 differs from these two features: neither is a βII' turn found with an internal hydrogen bond of Arg^1-NH to Asp^3-CO, nor is the backbone conformation around the γ turn highly flexible, which would cause strong deviations from the NMR data. However, the structure from the restrained MD simulation shows some minor deviations from the NOE and ROE intensities of the Gly^2 and Asp^3 amide protons. These deviations are indeed due to some flexibility as revealed by the free MD trajectory (Figure 4). During the simulation the largest deviation of the ϕ angle from the average value is found for glycine (±70°), while the corresponding deviations for arginine and phenylalanine are only about ±40°. The conformation of the glycine residue moves within the broad energy well around the C_7 conformer (see Brooks et al.[37] for the notation). The small violations of the NOE/ROE signals, Gly^2-H^N/Arg^1-H^β and Gly^2-H^N/Val^5-N(CH_3), can also be explained satisfactorily by a low percentage (below 10%) of another

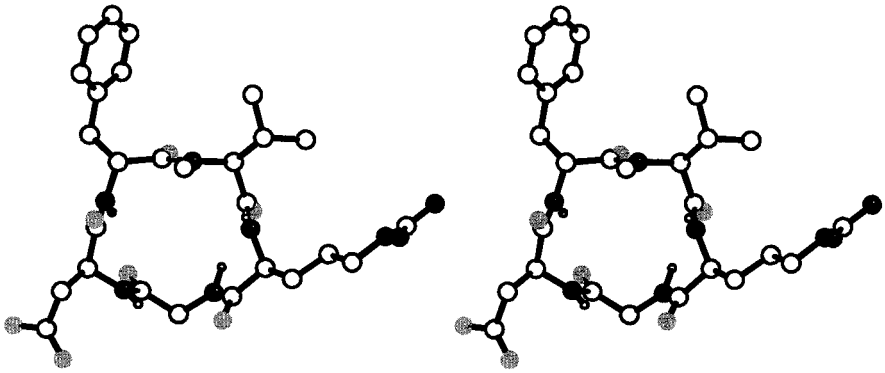

Figure 2. Stereoview of **P5** from the 100-ps restrained MD simulation, averaged and energy-minimized (20 steps conjugate gradient).

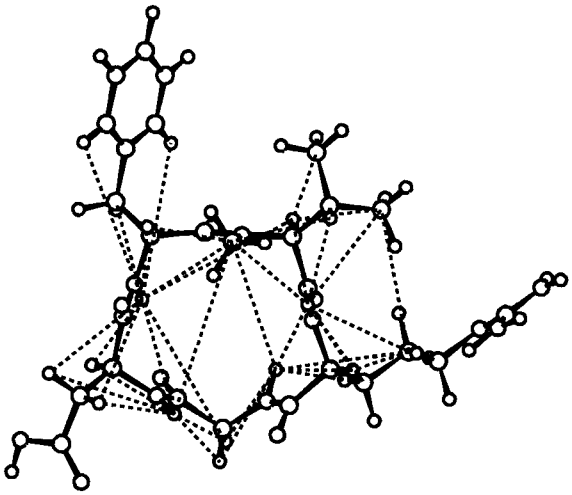

Figure 3. Illustration of the NOE/ROE-derived interproton distances which were used to determine the structure. Non-redundant NOE/ROE restraints are depicted as dashed lines. For methyl protons and degenerated methylene protons, the lines are connected to their corresponding carbon atom.

conformer in which the amide proton Gly^2-H^N points into the opposite direction of the peptide ring plane. This conformer would be realized by a flip of the amide group Arg^1-Gly^2, as is presumed to occur in other cyclic pentapeptides.[35,36] The flip can also be described as a shift of the arginine backbone from the energy well C_{7eq} to α_R and a glycine shift from C_7 toward the α_R region. The free MD simulation shows no flip of the amide group Arg^1-Gly^2 during the 400-ps trajectory, putting a lower limit on its orientational lifetime. An upper limit for the lifetime results from the fact that only one set of NMR signals is observed; i.e., all dynamic processes are efficiently averaged on the NMR time scale. Thus, the amide flip would occur on a time scale between ca. 10^{-9} and 10^{-1} s.

The structure of **P5** can be characterized by three turns, two γ_i turns with Arg^1 and Asp^3 at position $i+1$ and one γ turn with Gly^2 at $i+1$. According to the corresponding hydrogen bonds (Table 5) the turns are populated 36%, 15%, and 31%, respectively, during the free MD. The conformation from the restrained MD can be considered as the average conformation showing a distinct turn at arginine and a distorted turn at aspartate and glycine (Figure 2). All but the valine residue fall in the C_{7eq}/C_5 region of the Ramachandran plot similar to the bracelet structure of cyclic hexapeptides with alternating L,D-sequence where the orientation of the amide groups is also alternating and the $C^\alpha-C^\beta$ bonds are in an equatorial orientation with respect to the plane of the peptide ring.[38] The valine residue adopts the α_R conformation.

Temperature coefficients (Table 6), which are often considered a measure for the solvent accessibility of amide protons, must be interpreted carefully for **P5** in water. Here, they do not correlate with fast H_2O exchange as manifested by signal broadening of the amide protons at higher temperatures (Figure 5) and strong water exchange cross-peaks in the ROESY spectrum. The arginine amide proton shows the highest temperature shift indicating that it is not involved in a rigid hydrogen bond of a β turn which is found in the lead peptide **L1**. Taking into account both the temperature shift and the signal broadening, it is obvious that all of the amide protons are accessible to the solvent. Especially the protons Gly^2-H^N and Asp^3-H^N exchange fast with water due to the lack of a shielding side chain at the glycine residue. The strong line broadening also indicates that the $\gamma_i/\gamma/\gamma_i$ arrangement is flexible to some extent. Rigid turns with their corresponding hydrogen bonds should hinder the amide protons from exchange.

According to the $^3J(H^\alpha,H^\beta)$ coupling constants (Table 4) the side chains of the residues arginine, aspartate, and phenylalanine adopt mainly two different nearly equally populated rotamers, $\chi_1 = 180°/-60°$ for Arg^1 and Asp^3 and $\chi_1 = 180°/+60°$ for D-Phe^4, whereas the Val^5 side chain is predominantly anti-oriented. The rotation of side chains is fast on the NMR time scale but slow with respect to the CPU time required in order to sample adequately the populations during MD calculations. The 400-ps trajectory shows only a couple of changes between χ_1 rotamers. Considering the side chain orientations, the ensemble displayed in Figure 4 is therefore not representative.

We also measured **P5** in the solvent DMSO. Interestingly, DG structures calculated from the data in DMSO did not converge to a single conformation. None of the structures alone nor the whole ensemble of structures fulfilled the NMR data, implying that the peptide exhibits extensive conformational flexibility fast on the NMR time scale. Nevertheless, the DG structures with the lowest total error resemble those in water as they adopt a βII'-turnlike arrangement from Asp^3 to Arg^1 with perpendicular amide groups. They also show the highest conformational variability in the region around the glycine residue leading to the largest NOE viola-

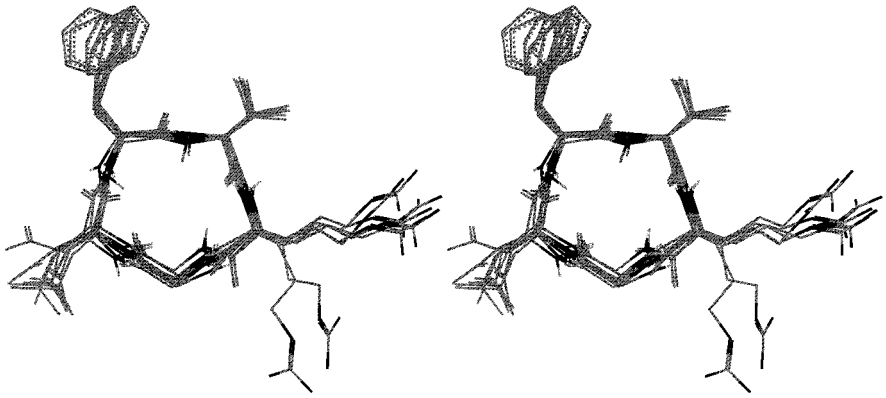

Figure 4. Superimposed conformations of **P5** sampled every 50 ps of the free MD trajectory.

Table 4. Experimental Coupling Constants (Hz) of **P5** in H_2O Compared to the Calculated Values from the Restrained and Free MD Simulations

	$^3J(H^N,H^\alpha)$			$^3J(H^\alpha,H^\beta)$
residue	exptl	rMD	fMD	exptl
Arg[1]	7.4	8.1[a]	8.0	7.5/7.5
Gly[2]	3.2[proR]	4.3[proR]	5.6[proR]	
	7.5[proS]	10.3[proS]	8.5[proS]	
Asp[3]	8.0	8.7	9.4	6.9[proR]
				8.0[proR]
D-Phe[4]	8.9	10.7[a]	9.8	6.8/9.0
Val[5]				10.8

[a] Coupling constant used as restraint in the rMD calculation.

Table 5. Population of the **P5** Hydrogen Bonds in H_2O during the Free MD Simulation[a]

donor	acceptor	population (%)
Gly[2] H^N	Val[5] CO	36
Asp[3] H^N	Arg[1] CO	31
Phe[4] H^N	Gly[2] CO	15
Arg[1] H^N	Asp[3] CO	0

[a] Hydrogen bonds are defined by a distance between acceptor and donor of $D_{A,D} \leq 2.8$ Å and an angle between the vectors CO and NH of $\delta = 180° \pm 60°$.

Table 6. Temperature Dependence of the Amide Proton Chemical Shift of *N*-Methylated Peptides in DMSO and **P5** in H_2O[a]

		amino acid				
no.	N(Me)-peptide	Arg[1]	Gly[2]	Asp[3]	D-Phe[4]	Val[5]
P1	[N(Me)Arg][1]		5.2	0.4	6.6	0.6
P2	[Sar][2]	5.0		2.7	3.7	2.7
P3	[N(Me)Asp][3]	3.9	4.0		−0.5	5.2
P4	[D-N(Me)Phe][4]	8.2	4.2	1.6		−0.9
P5	$[N(Me)Val]^5_{DMSO}$	5.7	0.7	4.0	5.4	
P5	$[N(Me)Val]^5_{H_2O}$	9.3	4.9	6.1	4.1	

[a] The coefficients are given in $-\Delta\delta/\Delta T$ (ppb/K) (parts per billion per K).

tions. The rms difference between the lowest error DG structure in DMSO and the averaged MD structure in H_2O is 0.43 Å for all backbone atoms and only 0.22 Å for the backbone not including the glycine residue and its adjacent peptide bonds. The structures in both solvents therefore resemble each other and differ mainly in the conformational flexibility around the γ turn.

Discussion

P5 is different from the other cyclic pentapeptides as the hydrogen bond formation between Arg[1]-H^N and Asp[3]-CO is blocked by the *N*-methyl group of the valine residue. Due to steric repulsion the amide groups Asp[3]-D-Phe[4] and Val[5]-Arg[1] turn into a more perpendicular orientation with respect to the plane of the peptide ring. As a result Arg[1] as well as Asp[3] adopt the C_{7eq} conformation. In other words, the two hydrogen bonds of the inverse γ turns, which compete with the γ turn at Gly[2], substitute for the one hydrogen bond formed in a βII' turn.

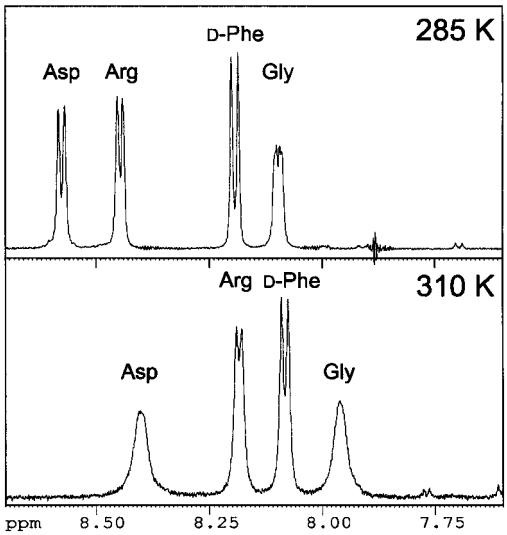

Figure 5. H^N region of the ^1H NMR (600 MHz, H_2O) spectra of **P5** measured at 285 and 310 K illustrating the different temperature shifts and line broadening.

The rotation of the peptide bonds Asp[3]-D-Phe[4] and Val[5]-Arg[1] moreover affects the side chains of Arg[1] and Asp[3] through allylic and vinylic strain, resulting in a pronounced conformational difference between **L1** and **P5** which certainly has an effect on the $\alpha_V\beta_3$ activity: While these side chains adopt a pseudoaxial position in **L1**, they are turned toward a more pseudoequatorial conformation in the *N*-methylated peptide. A strong kink of the RGD sequence, as characterized by a distance between the C_β atoms of Asp and Arg shorter than 6.7 Å, has been assumed to be vital for $\alpha_V\beta_3$ antagonist selectivity.[39] The results of this work are not in agreement with this assumption: The distance is 8.0 Å in the **P5** structure from the restrained MD simulation, and the average over the free MD trajectory is 8.5 Å. Even in the bound state, assuming an induced fit of the peptide, it is unlikely that the C_β atoms approach

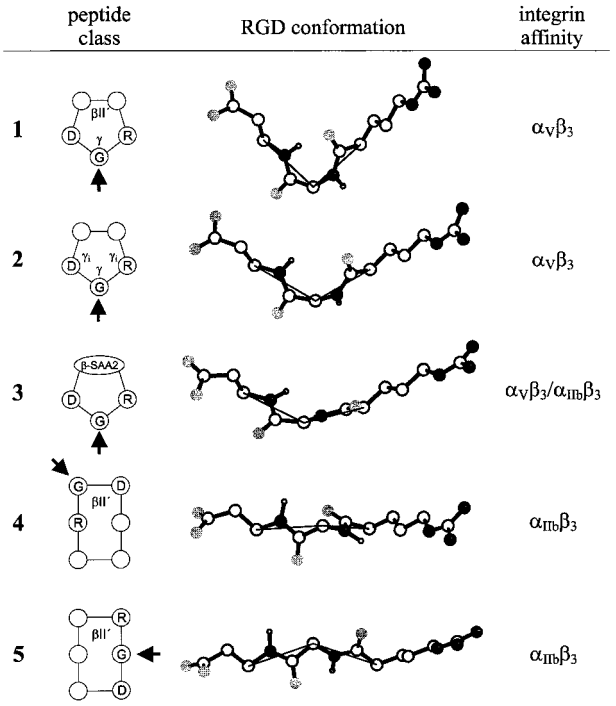

Figure 6. Illustration of different conformational requirements for $\alpha_V\beta_3$ and $\alpha_{IIb}\beta_3$ selectivity. Five classes of cyclic peptides and their representative RGD arrangements are shown, looking edge-on to the peptide ring (arrows indicate the line of sight). Only the RGD residues of the structures are displayed which are aligned with each other according to their $C^\alpha-C^\beta$ bonds. All side chains are shown in their anti-conformation. To emphasize the kink in the backbone, the C^α atoms are joined by a line.

each other as close as in **L1**; 7.1 Å is the very shortest distance measured during the 400-ps simulation at 300 K.

Although the RGD conformation is widened, there is still a distinct kink in the backbone which distinguishes **P5** from $\alpha_{IIb}\beta_3$-selective antagonists. Figure 6 illustrates the side-chain orientation and its effect on the receptor selectivity. Five classes of cyclic peptides are displayed along with a representative RGD conformation: **L1** represents class 1; **P5** represents class 2; the new class 3 is formed by peptides containing a sugar amino acid (SAA) that mimics a β turn, β-SAA2(Bn_3) in this example;[40] class 4 is represented by an ideal βII' turn conformation with Gly in the $i+1$ position; and the highly active compound cyclo(D-Abu-NMeArg-Gly-Asp-Mamb)[19] stands for class 5, respectively. Compounds of the first two classes are $\alpha_V\beta_3$-selective, while classes 4 and 5 show $\alpha_{IIb}\beta_3$-selectivity. The projection chosen for the RGD motif in Figure 6 clearly shows the difference in the kink angles which is responsible for the different selectivity.

Noteworthy, the class 3 peptide cyclo(Arg-Gly-Asp-β-SAA2(Bn_3)) exhibits an almost complete loss of selectivity ($IC_{50} = 0.025\ \mu M$ for $\alpha_V\beta_3$, $IC_{50} = 0.013\ \mu M$ for $\alpha_{IIb}\beta_3$). The conformation can easily be shifted toward both class 2 and class 5 by slight changes which can be engendered by the molecule's motion in solution or induced by the receptor. The high activity for both receptors suggests that the difference between the binding conformations is smaller than assumed until now and that a less kinked RGD structure is more optimal for the $\alpha_V\beta_3$ receptor selectivity, as in **P5**.

In addition to the orientation of the Arg and Asp side chains, the orientation of the amide groups adjacent to Gly certainly also plays an important role for inhibition. The loss of activity upon Gly-to-Ala substitution proves that a close contact between these two polar groups and the receptor is essential.[39] It is interesting to note that **P2** retains activity despite being *N*-methylated. Thus, it can be concluded that the *N*-methyl group in this case does not point outward, as with the C^α-methyl group in the Gly-to-Ala substitution, but rather lies perpendicular to the plane of the peptide ring. However, it is difficult to infer the proper orientation of these amide groups in the bound state from the known structures of cyclic RGD pentapeptides, since all active compounds show increased flexibility around Gly, facilitating conformational changes upon binding.

It is interesting to speculate that nature has used the flexibility around this glycine residue to develop receptor subtypes recognizing different RGD conformations. Since glycine allows for a greater variety of ϕ/ψ angle pairs, it is mainly the RGD vicinity in the protein which places conformational constraints on the arginine and aspartate moieties leading to a distinct orientation of these pharmacophoric groups relative to each other. In the same way the medicinal chemist can use conformational constraints induced by cyclization of small peptides to mimic nature's selectivity.

However, as long as no detailed three-dimensional structure of a RGD peptide or protein bound to the receptor is available, it is difficult to weigh the different contributions in substrates that are still flexible to a certain extent. So far, rather indirect conclusions for the design of new compounds can be drawn from such conformational SAR studies. Nevertheless, the search for constrained cyclic peptides led to the extremely potent **P5** which is now selected for development as a drug (code EMD121974) by Merck KGaA.

Conclusions

Each backbone amide bond of cyclo(RGDfV) (**L1**) was successively *N*-methylated to result in a series of five monomethylated cyclic pentapeptides. The influence of this *N*-methylation scan on biological activity was investigated and revealed cyclo(RGDf-N(Me)V-) (**P5**) as one of the most active and selective $\alpha_V\beta_3$ integrin antagonists known so far. The other four peptides showed lower activities, decreasing from **P1** to **P4**. In aqueous solution **P5** adopts a conformation characterized by a fast equilibrium between two inverse γ turns at Arg^1 and Asp^3 and a γ turn at Gly^2. The N(Me) group imparts steric repulsion via the peptide bonds Asp-D-Phe and Val-Arg leading to a less kinked orientation of the pharmacophoric center RGD which is probably closer to the binding conformation and hence attributes to the increased activity. It is apparent that a short distance between the C^β atoms of Arg and Asp is not necessarily a prerequisite for inhibiting $\alpha_V\beta_3$ integrins. Nevertheless, the kinked backbone is the most obvious feature that discriminates $\alpha_V\beta_3$ from $\alpha_{IIb}\beta_3$ antagonists.

Experimental Section

Materials and Methods. All chemicals were used as supplied without further purification. Apart from *N*-methylpyrrolidone (NMP) all organic solvents were distilled before use. Fmoc amino acids were purchased from Bachem (Heidel-

berg, Germany). cTrt resin was bought from CBL Patras (Patras, Greece), TBTU from Richelieu Biotechnologies (Montreal, Canada), HATU from Millipore (Bedford, Massachusetts), and HOAt from PerSeptive Biosystems (Hamburg, Germany). The *N*-methylated amino acids of D-Phe and Val were prepared as described by Freidinger et al.[26] Boc-N(Me)-Arg(Mtr)-OH was deprotected with HCl/ether, followed by protection with Fmoc-Cl under standard conditions.

NMR Spectroscopy. All spectra of the peptides **P1**−**P5** in DMSO-d_6 (as TFA salts) were obtained on a Bruker AMX500 spectrometer. The spectra were referenced relative to the residual DMSO signal (δ ^{1}H, 2.49 ppm; δ ^{13}C, 39.5 ppm). The spectra of peptide **P5** in H_2O (as its inner salt) were obtained on a Bruker DMX600 spectrometer. The sample concentration was 25 mM in a phosphate buffer at pH 6.0. The spectra were referenced relative to external DSS.[41] Water suppression was achieved using WATERGATE.[42] The assignment of all proton and carbon resonances was carried out using standard procedures.[43,44] Sequential assignment was accomplished by through-bond connectivities from heteronuclear multibond correlation (HMBC)[45−47] spectra. Proton distances were calculated using the two-spin approximation from nuclear Overhauser enhancement (NOESY)[48,49] or rotating frame nuclear Overhauser enhancement (ROESY)[50,51] spectra. Homonuclear coupling constants were determined from one-dimensional spectra and from PECOSY[52] cross-peaks. The temperature coefficients for the amide protons of each peptide were determined via ^{1}H spectra in the range 300−340 K with a step size of 10 K.

Computer Simulations. The structure calculations were performed on Silicon Graphics O2 R5000 and Origin R10000 computers. Metric matrix distance geometry calculations were carried out using a modified[53] version of DISGEO.[34,54] The DG procedure started with the embedding of 100 structures using random metrization.[55] For the refinement of the structures DISGEO employs distance- and angle-driven dynamics with NOE restraints and an additional ^3J-coupling potential[53] according to the Karplus equation. The MD calculations were carried out with the program DISCOVER using the CVFF force field.[56] The structure resulting from DG calculation was placed in a cubic box with a box length of 30 Å and soaked with H_2O. After energy minimization using steepest descent and conjugate gradient, the system was heated gradually starting from 50 K and increasing to 100, 150, 200, 250, and 300 K in 2-ps steps, each by direct scaling of velocities. The system was equilibrated for 20 ps with temperature bath coupling (300 K). Configurations were saved every 100 fs for another 100 ps. The free MD simulation started from the end of the restrained MD with an equilibration of 40 ps.

Biological Assay. 1. Protein Purification. Human plasma vitronectin[57] and fibrinogen[58] were purified as described previously. $\alpha_V\beta_3$ integrin was purified from human placenta[59] with modifications,[60] using antibody affinity chromatography on an LM609 antibody column. $\alpha_{IIb}\beta_3$ integrin was prepared by peptide affinity chromatography from human platelets[61] with modifications,[60] using a linear GRGDSPK-conjugated CL-4B Sepharose column. Both preparations were ∼95% pure as judged by antiintegrin ELISA using α and β chain-specific monoclonal antibodies and by SDS−PAGE.

2. Isolated Integrin Binding Assays. Inhibitory effects of cyclic peptides were quantified by measuring their effect on the interactions between immobilized integrin and biotinylated soluble ligands. Purified vitronectin or fibrinogen (1 mg/mL; pH 8.2) was biotinylated with *N*-hydroxysuccinimidobiotin (100 μg/mL; 1 h, 20 °C), before dialysis into PBS. Integrins diluted to 1 μg/mL (∼1:1000 dilution of stock) were adsorbed to 96-well nontissue culture-treated microtiter plates. After blocking of free protein binding sites, biotinylated ECM ligand at 1 μg/mL was added and incubation continued at 37 °C for 3 h. Unbound ligand was washed away and bound biotin detected with alkaline-phosphate-conjugated antibiotin antibodies. For peptide competition assays, peptides were serially diluted before addition to integrin-coated wells, followed by co-incubation with biotinylated ligand and detection as described above. Assays were performed in triplicate, the mean binding values were fitted to a sigmoid, and the IC_{50} was derived. Values shown represent the mean of at least three separate determinations of IC_{50}. External standards of linear GRGDSPK and cyclo(RGDfV) were routinely included to monitor the dynamic range and the stability of the assay.

Supporting Information Available: Data from HPLC and HRMS spectra of the *N*-methylated peptides **P1**−**P5**. This material is available free of charge via the Internet at http://pubs.acs.org.

References

(1) Aumailley, M.; Gurrath, M.; Müller, G.; Calvete, J.; Timpl, R.; Kessler, H. Arg-Gly-Asp Constrained within Cyclic Pentapeptides. Strong and Selective Inhibitors of Cell Adhesion to Vitronectin and Laminin Fragment P1. *FEBS Lett.* **1991**, *291*, 50−54.

(2) Gurrath, M.; Müller, G.; Kessler, H.; Aumailley, M.; Timpl, R. Conformation/Activity Studies of Rationally Designed Potent Anti-Adhesive RGD Peptides. *Eur. J. Biochem.* **1992**, *210*, 911−921.

(3) Müller, G.; Gurrath, M.; Kessler, H.; Timpl, R. Dynamic Forcing, a Method for Evaluating Activity and Selectivity Profiles of RGD Peptides. *Angew. Chem., Int. Ed. Engl.* **1992**, *31*, 326−328.

(4) Kessler, H.; Gratias, R.; Hessler, G.; Gurrath, M.; Müller, G. Conformation of Cyclic Peptides. Principle Concepts and the Design of Selectivity and Superactivity in Bioactive Sequences by "Spatial Screening". *Pure Appl. Chem.* **1996**, *68*, 1201−1205.

(5) Kessler, H.; Diefenbach, B.; Finsinger, D.; Geyer, A.; Gurrath, M.; Goodman, S. L.; Hölzemann, G.; Haubner, R.; Jonczyk, A.; Müller, G.; von Roedern, E. G.; Wermuth, J. Design of Superactive and Selective Integrin Receptor Antagonists Containing the RGD Sequence. *Lett. Pept. Sci.* **1995**, *2*, 155−160.

(6) Haubner, R.; Gratias, R.; Diefenbach, B.; Goodman, S. L.; Jonczyk, A.; Kessler, H. Structural and Functional Aspects of RGD-Containing Cyclic Pentapeptides as Highly Potent and Selective Integrin $\alpha_V\beta_3$ Antagonists. *J. Am. Chem. Soc.* **1996**, *118*, 7461−7472.

(7) Wermuth, J.; Goodman, S. L.; Jonczyk, A.; Kessler, H. Stereoisomerism and Biological Activity of the Selective and Superactive $\alpha_V\beta_3$ Integrin Inhibitor cyclo(−RGDfV-) and Its Retro-Inverso Peptide. *J. Am. Chem. Soc.* **1997**, *119*, 1328−1335.

(8) Haubner, R.; Schmitt, W.; Hölzemann, G.; Goodman, S. L.; Jonczyk, A.; Kessler, H. Cyclic RGD Peptides Containing β-Turn Mimetics. *J. Am. Chem. Soc.* **1996**, *118*, 7881−7891.

(9) Haubner, R.; Finsinger, D.; Kessler, H. Stereoisomeric Peptide Libraries and Peptidomimetics for Designing Selective Inhibitors of the $\alpha_V\beta_3$ Integrin for a New Cancer Therapy. *Angew. Chem., Int. Ed. Engl.* **1997**, *36*, 1374−1389.

(10) Keenan, R. M.; Miller, W. H.; Kwon, C.; Ali, F. E.; Callahan, J. F.; Calvo, R. R.; Hwang, S. M.; Kopple, K. D.; Peishoff, C. E.; Samanen, J. M.; Wong, A. S.; Yuan, C. K.; Huffman, W. F. Discovery of Potent Nonpeptide Vitronectin Receptor ($\alpha_V\beta_3$) Antagonists. *J. Med. Chem.* **1997**, *40*, 2289−2292.

(11) Brooks, P. C.; Montgomery, A. M. P.; Rosenfeld, M.; Reisfeld, R. A.; Hu, T.; Klier, G.; Cheresh, D. A. Integrin $\alpha_V\beta_3$ Antagonists Promote Tumor Regression by Inducing Apoptosis of Angiogenetic Blood Vessels. *Cell* **1994**, *79*, 1157−1164.

(12) Montgomery, A. M. P.; Reisfeld, R. A.; Cheresh, D. A. Integrin-$\alpha_V\beta_3$ Rescues Melanoma Cells from Apoptosis in 3-Dimensional Dermal Collagen. *Proc. Natl. Acad. Sci. U.S.A.* **1994**, *91*, 8856−8860.

(13) Ruoslahti, E.; Reed, J. C. Anchorage Dependence, Integrins and Apoptosis. *Cell* **1994**, *77*, 477−478.

(14) Albelda, S. M.; Mette, S. A.; Elder, D. E.; Stewart, R. M.; Damjanovich, L.; Herlyn, M.; Buck, C. A. Integrin Distribution in Malignant-Melanoma-Association of the β_3−Subunit with Tumor Progression. *Cancer Res.* **1990**, *50*, 6757−6764.

(15) Zutter, M. M.; Krigman, H. R.; Santoro, S. A. Altered Integrin Expression in Adenocarcinoma of the Breast. *Am. J. Pathol.* **1993**, *142*, 1439−1448.

(16) Manavalan, P.; Momany, F. A. Conformational Energy Studies on *N*-Methylated Analogues of Thyrotropin Releasing Hormone, Enkephalin and Luteinizing Hormone Releasing Hormone. *Biochemistry* **1980**, *19*, 1943−1973.

(17) Tonelli, A. E. The Effects of Isolated *N*-Methylated Residues on the Conformational Characteristics of Polypeptides. *Biopolymers* **1976**, *15*, 1615−1622.

(18) Ron, D.; Gilon, C.; Hanani, M.; Vromen, A.; Selinger, Z.; Chorev, M. *N*-Methylated Analogues of Ac[Nle28,31]CCK(26−33). *J. Med. Chem.* **1992**, *35*, 2806−2811.

(19) Bach II, A. C.; Eyermann, C. J.; Gross, J. D.; Bower, M. J.; Harlow, R. L.; Weber, P. C.; DeGrado, W. F. Structural Studies of a Family of High Affinity Ligands for GPIIb/IIIa. *J. Am. Chem. Soc.* **1994**, *116*, 3207−3219.

(20) Mazur, R. H.; James, P. A.; Tyner, D. A.; Hallinan, E. A.; Sanner, J. H.; Schulze, R. J. Bradykinin Analogues Containing N^{α}-Methyl Amino Acids. *J. Med. Chem.* **1980**, *23*, 758−763.
(21) Haviv, F.; Fitzpatrick, T. D.; Swenson, R. E.; Nichols, C. J.; Mort, N. A.; Bush, E. N.; Diaz, G.; Bammert, G.; Nguyen, A.; Rhutasel, N. S.; Nellans, H. N.; Hoffman, D. J.; Johnson, E. S.; Greer, J. Effect of *N*-Methyl Substitution of the Peptide-Bonds in Luteinizing Hormone Releasing Hormone Agonists. *J. Med. Chem.* **1993**, *36*, 363−369.
(22) Wormser, U.; Laufer, R.; Hart, Y.; Chorev, M.; Gilon, C.; Selinger, Z. Highly Selective Agonists for Substance P Receptor Subtypes. *EMBO J.* **1986**, *5*, 2805−2808.
(23) Bach II, A. C.; Espina, J. R.; Jackson, S. A.; Stouten, P. F. W.; Duke, J. L.; Mousa, S. A.; DeGrado, W. F. Type II′ to Type I β-Turn Swap Changes Specificity for Integrins. *J. Am. Chem. Soc.* **1996**, *118*, 293−294.
(24) McDermott, J. R.; Benoiton, N. L. *N*-Methylamino Acids in Peptide Synthesis. A New Synthesis of *N*-Benzyloxycarbonyl, *N*-Methylamino Acids. *Can. J. Chem.* **1973**, *51*, 1915−1919.
(25) Cheung, S. T.; Benoiton, N. L. *N*-Methylamino Acids in Peptide Synthesis. *Can. J. Chem.* **1977**, *55*, 916−921.
(26) Freidinger, R. M.; Hinkle, J. S.; Perlow, D. S.; Arison, B. H. Synthesis of 9-Fluorenylmethyloxycarbonyl-Protected N-Alkyl Amino Acids by Reduction of Oxazolidinones. *J. Org. Chem.* **1983**, *48*, 77−81.
(27) Merrifield, R. B. Solid-Phase Peptide Synthesis. *J. Am. Chem. Soc.* **1963**, *85*, 2149−2154.
(28) Merrifield, R. B. Solid-Phase Synthesis. *Angew. Chem., Int. Ed. Engl.* **1985**, *24*, 799−810.
(29) Fields, G. B.; Noble, R. L. Solid-Phase Peptide Synthesis Utilizing 9-Fluorenylmethoxycarbonyl Amino Acids. *Int. J. Pept. Prot. Res.* **1990**, *35*, 161−214.
(30) Brady, S. F.; Paleveda, W. J.; Arison, B. H.; Freidinger, R. M.; Nutt, R. F.; Veber, D. F. An Improved Procedure for Peptide Cyclization. In *Peptides: Structure and Function. Proceedings of the 8th American Peptide Symposium*; Hruby, V. J., Rich, D. H., Eds.; Pierce Chemical Co.: Rockford, IL, 1983; pp 127−130.
(31) Simon, R. J.; Kania, R. S.; Zuckermann, R. N.; Huebner, V. D.; Jewell, D. A.; Banville, S.; Ng, S.; Wang, L.; Rosenberg, S.; Marlowe, C. K.; Spellmeyer, D. C.; Tan, R.; Frankel, A. D.; Santi, D. V.; Cohen, F. E.; Bartlett, P. A. Peptoids: A Modular Approach to Drug Discovery. *Proc. Natl. Acad. Sci. U.S.A* **1992**, *89*, 9367−9371.
(32) Ali, F. E.; Calvo, R.; Romoff, T.; Samanen, J.; Nichols, A.; Store, B. Structure−Activity Studies toward the Improvement of Antiaggregatory Activity of RGDS. In *Peptides: Chemistry, Structure and Biology*, Rivier, J. E., Marshall, G. R., Eds.; ESCOM Science: Leiden (The Netherlands), 1990; pp 94−96.
(33) Fletcher, C. M.; Jones, D. N. M.; Diamond, R.; Neuhaus, D. Treatment of NOE Constraints Involving Equivalent or Nonstereoassigned Protons in Calculations of Biomacromolecular Structures. *J. Biol. NMR* **1996**, *8*, 292−310.
(34) Havel, T. F. An Evaluation of Computational Strategies for Use in the Determination of Protein Structure from Distance Constraints Obtained by Nuclear Magnetic Resonance. *Prog. Biophys. Mol. Biol.* **1991**, *56*, 43−78.
(35) Koppitz, M.; Huenges, M.; Gratias, R.; Kessler, H.; Goodman, S. L.; Jonczyk, A. Synthesis of Unnatural Lipophilic N-(9H-Fluoren-9-ylmethoxy)carbonyl-Substituted α-Amino Acids and Their Incorporation into Cyclic RGD-Peptides: A Structure−Activity Study. *Helv. Chim. Acta* **1997**, *80*, 1280−1300.
(36) Mierke, D. F.; Kurz, M.; Kessler, H. Peptide Flexibility and Calculation of an Ensemble of Molecules. *J. Am. Chem. Soc.* **1994**, *116*, 1042−1049.
(37) Brooks, C. L. I.; Case, D. A. Simulations of Peptide Conformational Dynamics and Thermodynamics. *Chem. Rev.* **1993**, *93*, 2487−2502.
(38) Pavone, V.; Benedetti, E.; Di Blasio, B.; Lombardi, A.; Pedone, C. Regularly Alternating L,D-Peptides. III. Hexacyclic Peptides from Valine or Phenylalanine. *Biopolymers* **1989**, *28*, 215−223.
(39) Pfaff, M.; Tangemann, K.; Müller, B.; Gurrath, M.; Müller, G.; Kessler, H.; Engel, R. T. J. Selective Recognition of Cyclic RGD Peptides of NMR Defined Conformation by $\alpha_{IIb}\beta_3$, $\alpha_v\beta_3$, and $\alpha_5\beta_1$ Integrins. *J. Biol. Chem.* **1994**, *269*, 20233−20238.
(40) Lohof, E.; Burkhart, F.; Planker, E.; Mang, C.; Dechantsreiter, M. A.; Hölzemann, G.; Goodman, S.; Kessler, H. Unpublished results.
(41) Wishart, D. S.; Bigam, C. G.; Yao, J.; Abildgaard, F.; Dyson, H. J.; Oldfield, E.; Markley, J. L.; Sykes, B. D. ^{1}H, ^{13}C and ^{15}N Chemical Shift Referencing in Biomolecular NMR. *J. Biomol. NMR* **1995**, *6*, 135−140.
(42) Piotto, M.; Saudek, V.; Sklenar, V. Gradient-Tailored Excitation for Single-Quantum NMR Spectroscopy of Aqueous Solution. *J. Biomol. NMR* **1992**, *2*, 661−666.
(43) Kessler, H.; Schmitt, W. In *Encyclopedia of Nuclear Magnetic Resonance*; Grant, D. M., Harris, R. K., Eds.; J. Wiley & Sons: New York, 1996; Vol. 6, 3527−3537.
(44) Kessler, H.; Seip, S. In *Two-Dimensional NMR−Spectroscopy, Applications for Chemists and Biochemists*; Croasmun, W. R., Carlson, M. K., Eds.; VCH Publishers: New York, 1994; pp 619−654.
(45) Bax, A.; Summers, M. F. ^{1}H and ^{13}C Assignments from Sensitivity-Enhanced Detection of Heteronuclear Multiple-Bond Connectivity by 2D Multiple Quantum NMR. *J. Am. Chem. Soc.* **1986**, *108*, 2093−2094.
(46) Bermel, W.; Wagner, K.; Griesinger, C. Proton-Detected C,H Correlation via Long-Range Couplings with Soft Pulses; Determination of Coupling Constants. *J. Magn. Reson.* **1989**, *83*, 223−232.
(47) Kessler, H.; Schmieder, P.; Köck, M.; Kurz, M. Improved Resolution in Proton-Detected Heteronuclear Long-Range Correlation. *J. Magn. Reson.* **1990**, *88*, 615−618.
(48) Jeener, J.; Meier, B. H.; Bachmann, P.; Ernst, R. R. *J. Chem. Phys* **1979**, *71*, 4546−4553.
(49) Wüthrich, K. In *NMR of Proteins and Nuclei Acids*; Wiley & Sons: New York, 1986.
(50) Bothner-By, A. A.; Stevens, R. L.; Lee, J.; Warren, C. D.; Jeanloz, R. W. Structure Determination of a Tetrasaccharide: Transient Nuclear Overhauser Effects in the Rotating Frame. *J. Am. Chem. Soc.* **1984**, *106*, 811−813.
(51) Kessler; Griesinger, C.; Kerssebaum, R.; Wagner, K.; Ernst, R. R. Separation of Cross-Relaxation and J Cross-Peaks in 2D Rotating Frame NMR Spectroscopy. *J. Am. Chem. Soc.* **1987**, *109*, 607−609.
(52) Mueller, L. P. E. COSY. A Simple Alternative to E. COSY. *J. Magn. Reson.* **1987**, *72*, 191−196.
(53) Mierke, D. F.; Kessler, H. Improved Molecular Dynamics Simulations for the Determination of Peptide Structures. *Biopolymers* **1993**, *33*, 1003−1017.
(54) Havel, T. F. DISGEO. Quantum Chemistry Exchange Program 1988, Exchange No. 507, Indiana Univeristy.
(55) Havel, T. F. The Sampling Properties of Some Distance Geometry Algorithms Applied to Unconstrained Polypeptide Chains: A Study of 1830 Independently Computed Conformations. *Biopolymers* **1990**, *29*, 1565−1585.
(56) Hagler, A. F.; Lifson, S.; Dauber, P. Consistent Force Field Studies of Intermolecular Forces in Hydrogen-Bonded Crystals. *J. Am. Chem. Soc.* **1979**, *101*, 5122−5130.
(57) Yatohgo, T.; Izumi, M.; Kashiwagi, H.; Hayashi, M. Novel Purification of Vitronectin from Human-Plasma by Heparin Affinity-Chromatography. *Cell Struct. Funct.* **1988**, *13*, 281−292.
(58) Kazal, L. A.; Ansel, S.; Miller, O. P.; Tocantins, L. M. *Proc. Soc. Exp. Biol. Med.* **1963**, *113*, 989−994.
(59) Smith, J. W.; Cheresh, D. A. The Arg-Gly-Asp Binding Domain of the Vitronectin Receptor. *J. Biol. Chem.* **1988**, *263*, 18726−18731.
(60) Mitjans, F. C.; Sander, D.; Adán, J.; Sutter, A.; Martinez, J. M.; Jäggle, C.; Moyano, J. M.; Kreysch, H.; Piulats, J.; Goodman, S. L. An Anti-α_V-Integrin Antibody that Blocks Integrin Function Inhibits the Development of a Human-Melanoma in Nude-Mice. *Cell Sci.* **1995**, *108*, 2825−2838.
(61) Pytela, R.; Pierschbacher, M. D.; Ginsberg, M. H.; Plow, E. F.; Ruoslahti, E. Platelet Membrane Glycoprotein IIb/IIIa-Member of a Family of Arg-Gly-Asp Specific Adhesion Receptors. *Science* **1986**, *231*, 1559−1562.

JM970832G